

Article

An Improved Evaluation Strategy for Ash Analysis Using Scanning Electron Microscope Automated Mineralogy

Andrea C. Guhl ¹, Valentin-G. Greb ¹, Bernhard Schulz ² and Martin Bertau ^{1,*}

¹ TU Bergakademie Freiberg, Institute of Chemical Technology, Leipziger Straße 29, 09599 Freiberg, Germany; andrea.guhl@chemie.tu-freiberg.de (A.C.G.); valentin.greb@alba.info (V.-G.G.)

² TU Bergakademie Freiberg, Institute of Mineralogy, Brennhausgasse 14, 09599 Freiberg, Germany; bernhard.schulz@mineral.tu-freiberg.de

* Correspondence: martin.bertau@chemie.tu-freiberg.de

Received: 31 March 2020; Accepted: 20 May 2020; Published: 25 May 2020



Abstract: Sewage slush ashes are materials composed of polyphase particles. Ashes are fine-grained with many amorphous components, and analytical techniques such as X-ray diffractometry cannot recover all the properties. For sewage sludge ash, treatment often focuses on phosphate recovery. Automated mineralogy techniques were applied in order to study phosphate associations and their behavior towards chemical processes. This work shows the distribution of phosphate content in sewage sludge ash and identifies the main recovered phosphate phases in acid leaching. Data interpretation was focused on the target material, phosphate. The approach documents spectra labelling with respect to one target component, phosphorus. This is a tool for assessing sewage sludge ashes towards their phosphate recovery potential and highlights issues processing needs to address.

Keywords: sewage sludge ashes (SSA); phosphate; recycling; recovery; SEM-automated mineralogy; mineral liberation analysis (MLA)

1. Introduction

In 2014, the European Commission published a document on critical raw materials, including phosphate [1]. In conjunction with the circular economy initiative of the European Commission, the waste management sector started working on commodity recovery from materials previously regarded as disposable. Thereby, the term “resources” was widened from ores to include industrial ashes. Several countries are incinerating sewage sludge, as previous disposal choices are no longer an option legally [2]. The resulting sewage sludge ash (SSA) is now the product workers are focusing P-recovery techniques on (e.g., [3–8]). SSA is not only complex in composition, but also diverse (depending on provenance, incineration parameters and other factors). In order to optimize recovery techniques, the P-content (target) needs exploring. Here, strategies from primary resources may help. This paper follows previous work [9–11] and adds insights from scanning electron microscopy-based automated mineralogy (SEM-AM) work, a technique from primary resources, to this waste management issue. A number of systems are available among this group, such as QEMSCAN, Mineralogic, TIMA (TESCAN Integrated Mineral Analyzer) and MLA (Mineral Liberation Analyzer).

Knowing both particle morphology as well as composition is an advantage in devising technologies to extract a targeted component from a diverse material. Addressing these issues, the MLA by FEI, Inc. was chosen to study SSA particles with an SEM-AM system [12]. This offers a complete phase analysis (definitive array of minerals), as well as information about the X-ray amorphous components. Since current approaches to evaluating these datasets aim at identifying minerals among the EDX

spectra [13–15], and SSA do not consist of known minerals only, the evaluation of datasets needed some adjustments [16]. Here, we present an approach to complex material investigation using SEM-MLA.

2. Materials and Methods

2.1. Materials

SSA investigated originates from a sewage sludge mono-combustion plant that was kindly provided by “Wirbelschichtfeuerungsanlage Elverlingsen GmbH”, 58791 Werdohl-Elverlingsen, Germany. All chemicals were supplied by Merck KGaA, Darmstadt, Germany. Reactants used were HCl, reagent grade 36.5% (used 493.2 g and diluted to 1 L in a volumetric flask with distilled water to prepare 5.0 M) and NH₄Cl. Epo-TEK by Epoxy Technology Inc., Billerica, MA, USA was supplied by Logitech Ltd., Glasgow, UK.

2.2. Methods

The methods used are acid digestion, thermochemical treatment of SSA and MLA investigation. SSA was subjected to digestion. Digestion was carried out by adding inorganic acid (HCl (5 N)) for 5 min at ambient temperature. The amount of solids was 5 g sample and 20 g acid. This was done in a beaker while stirring permanently. Following digestion, cake washing with distilled water was carried out using 2 × 50 mL. The resulting residue was dried at 110 °C for 2 h in a drying cabinet.

Then, acid digestion was undertaken after thermochemical pre-treatment: SSA was mixed with NH₄Cl at a ratio of 1:1 and heated in a kiln. A first temperature rest was kept for 2 h at 250 °C, then another rest was kept for 2 h at 350 °C. Finally, the material was heated to 1000 °C in order to remove the remaining heavy metal volatiles. A continuous inert gas flow of N₂ was applied at 15 L/h. Afterwards, the material was processed using inorganic acid (HCl (5 N)) at a digestion time of 5 min without additional heating and a liquid/solid ratio of 4:1. Both processes were accompanied by sampling for SEM-MLA investigation.

Three powder samples were collected: (i) untreated SSA; (ii) digested, rinsed and dried SSA residue; (iii) thermochemically treated, digested, rinsed and dried SSA residue. These samples were prepared and subjected to the grain mount preparation procedure. Preparation included mixing the dried sample powder 1:1 with graphite (for particle separation) and stirring this mix into epoxy in Teflon containers with 30 mm in diameter. Epoxy blocks were generated, whetted, polished and carbon coated for measurement. The samples were introduced into the vacuum chamber of the SEM and beam acceleration was set at 25 kV with a current of 10 nA; horizontal frame width (HWF) set to 373 pixels. For the acquisition of the grey-scale BSE image, Cu was selected as the BSE grey-scale standard (materials with a Z value of Cu or higher appear as 256 (very bright), all other material turn out darker, respectively). Spectral data were obtained using the GXMAP procedure, that is, particles are automatically detected and covered with a grid of measurement points [12]. Particles smaller than 20 pixels were identified by a single measurement point. Fractions of the sample are given in area-% in this work, since the density of SSA material is difficult to assess. Keeping proportions representative, densities (even of known minerals) were set to one, so “% of the sample” refers to area-% (data were gathered from a polished surface, the actual measurement was that of an area). Proportions of the elemental contents in spectra are weight-%, thus, shares of phosphorus within the material are wt%.

In this study, sewage sludge ashes are analyzed with respect to their P-content and treated SSA checked for residual P-content. For data evaluation, a new approach to sorting and handling EDX spectra is applied. Similarly, workers have previously adapted data evaluation strategies, such as Ayling et al., 2012 [17] devising a new species identification protocol. A similar target-element focused evaluation using QEMSCAN to investigate eudialyte residue has been reported by Ma et al., 2018 [18]. The target component labelling looks at the P-content according to each spectrum and allows for a target material grouping. Conventionally, a mineral grain or particle is classified by comparing the collected EDX spectra to a set of reference spectra labelled by mineral names. EDX spectra of SSA are

complex, with a multitude of peaks for Si, Al, Ca, Fe, S and P at various counts (97.6 area-% of the material is comprised of these and oxygen). Other elements found are Ba, Cl, Cr, Cu, K, Mg, Mn, Na and Ti. Due to small grain sizes and transitions between grains of different compositions, there are also some “mixed” spectra which display a combination of peaks from elements in adjacent grains. These conditions, in addition to amorphous, artificially produced material phases, render an interpretation of the spectra as a mineral impossible and do not allow for spectra labelling with mineral names. Using EDX-elemental analysis for quantifying the Si, Al, Ca, Fe, S and P-contents, 53 spectra were collected from the samples, which were then used as reference spectra for classifying the samples. For such reference spectra, generic labelling [16] is a viable approach.

Subsequently, these reference spectra are sorted by their P-content. Spectra groups summarizing the spectra within a range of P-contents (in wt%) are then named descriptively, “<1% P” or “5–10% P”, for example (Table 1). This step is called the target component grouping. There is an interesting tendency of elemental complexity (number of elements detected) decreasing as P-content rises. In phosphate recycling, recovering a few other elements in addition to P is desirable as it reduces the need for product purification. The procedure differs from the other ways of grouping by sorts of minerals [16], as it focuses on a single elemental component in amorphous particles. All software operations used MLA datasuite 3.1.4.686.

Table 1. Target component grouping—number of spectra and elemental complexity in each group.

Group	Number of Spectra	Comment
<1% P	13	often mixed spectra
1–5% P	9	On average, composed of 9.66 distinct elements
5–10% P	4	On average, composed of 9.75 distinct elements
10–15% P	4	On average, composed of 7 distinct elements
>15% P	2	On average, composed of 6 distinct elements
3 key	3	completely removed by acid digestion, not present in residues; on average, 7.33 distinct elements

Non-P-containing material components are quartz and other silica-rich species, calcium sulphate spectra, iron oxides and residuals/erroneous identification. The GXMAP measurements were classified against the reference EDX-ray spectra list using the MLA 3.1.4 software version. All spectra were collected with 11,000 counts minimum, with an error level of 0.5% or less. Thereby, this method tries to meet the general accuracy challenges of EDX with statistical significance. Less than 0.6% of the sample area remained classified as unknown, with no X-ray counts, or as unspecified due to a low number of counts. Not all phases have been detected in amounts of relevance. These were grouped as others. The arbitrary cut-off value (below—others, above—relevant compositional phase) is 0.4 area-%. For “BaCaO”, the percentage is <0.3 area-% of the sample, represented by <1400 grains. All other spectra are below these values, and thus, only secondary in relevance. As an area was measured, values of percentages refer to area-% unless otherwise noted.

3. Results

While the MLA software package offers several options for exploring data, not all are suited to study SSA. The locking operation offers insights into preferential association of material phases, e.g., how a certain component forms particles with other material phases. This encompasses preferential partner species in multi-material particles as well as the degree of liberated (mono-material) particles. Another function, calculated assay, gives a rough estimate of the elemental composition of the whole sample. This is used as a relative function to see trends, in the case here, P-content of SSA (6%) dropped to 0.5% in acid residue after.

The other operation deemed applicable here is chemical composition of the material as based on EDX spectra. Unlike X-ray diffractometry (XRD) measurements, which are only applicable to the crystalline portion of the sample, this technique yields information about the whole sample (including

amorphous material). In addition, XRD measurements of this material suffer from peak shifting due to the considerable portion of amorphous material and hardly any clearly developed peaks. Initial endeavors to fit EDX-derived material phases to XRD-derived mineral phases were only able to determine quartz. The reflexes of known phosphorus minerals (whitlockite, apatite, etc.) are not developed in the XRD spectra. This is interpreted as one of two modes: (1) P-phases in this SSA are present as a yet unknown mineral, or (2) the P-content of SSA is largely present within the amorphous part of the material. As Table 1 lists, phosphate-bearing components found in SSA contain more than just Ca, P and O. For P-recovery, secondary resource users are interested in phases with low complexity and as few elements as possible. During phosphoric acid production, these other elements would necessitate purification, an elaborate and costly process. As P-content rises, the complexity of phases decreases. Thus, it might be interesting to focus on high P portions of SSA in recovery in order to lower purification cost. The general appearance of this SSA prior to chemical treatment is reflected in the BSE images in Figure 1. In the following, particles are discussed. Particles in this material are either inherited—they existed prior to combustion—or a product of incineration processes.

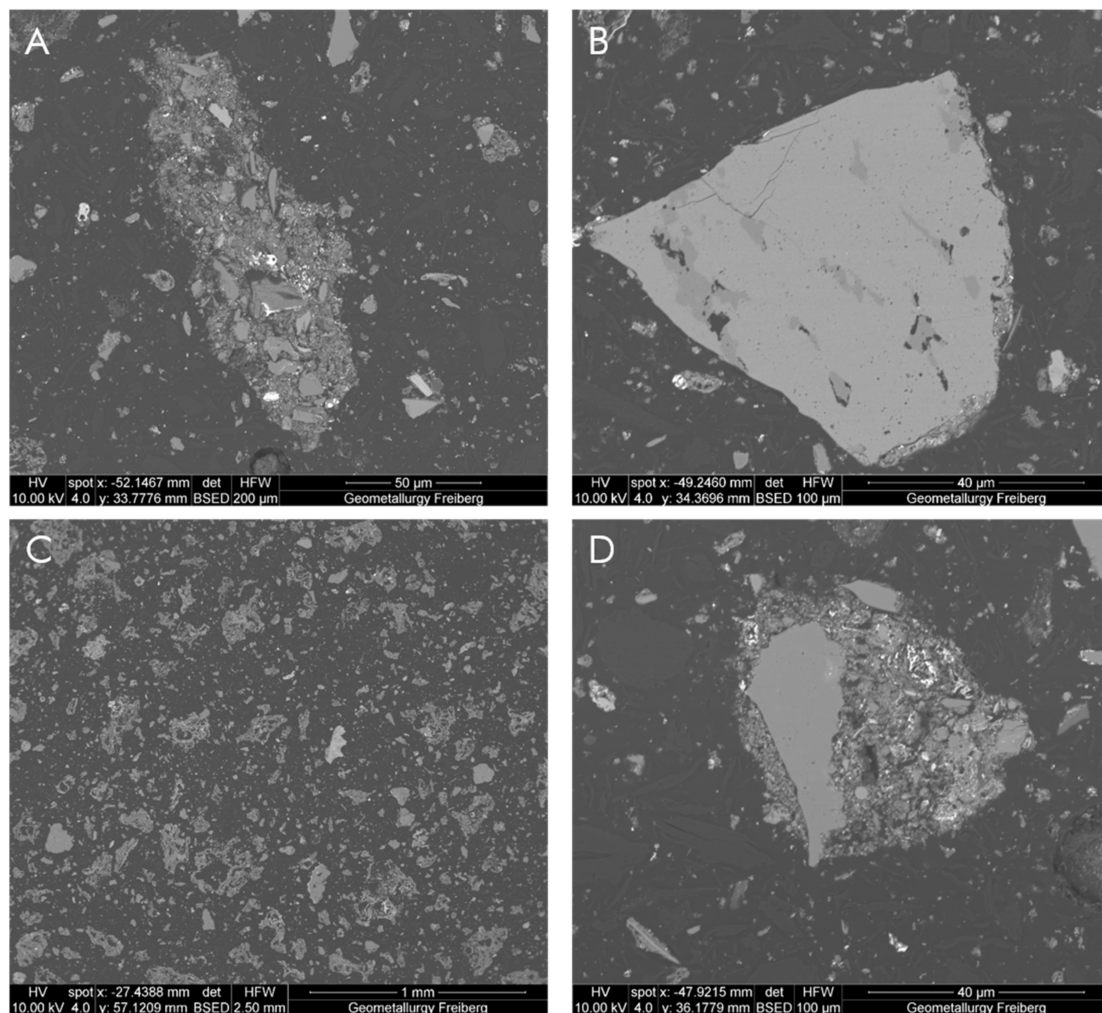


Figure 1. BSE images of sewage sludge ash mixed with graphite for particle separation and stabilized with epoxy for analysis. (A) agglomeration of fine flakes; (B) inherited mineral grain, presumably from fluidized bed, bottom right of the grain shows P-rich material condensing onto grain; (C) general overview of SSA and (D) agglomeration around inherited grain.

Using the target component grouping subsequent to a generic labelling approach [16], the material composition of three samples is shown. Figure 2 compares the initial ash, digestion residue after HCl treatment, and digestion residue after thermochemical pre-treatment.

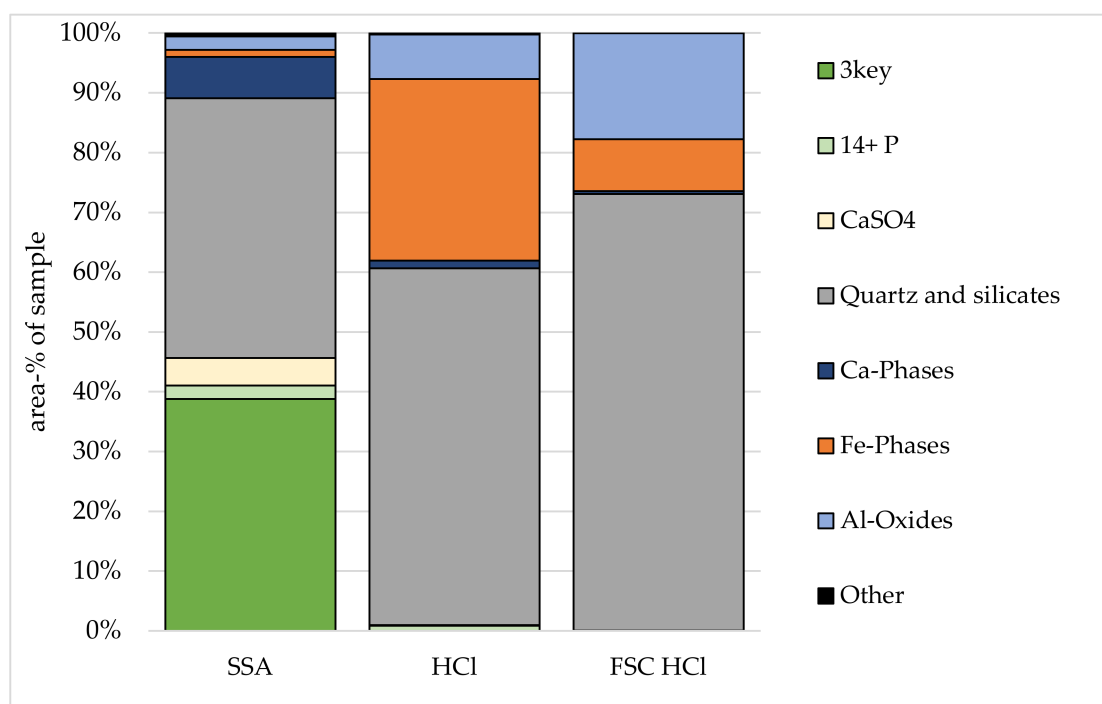


Figure 2. Composition of untreated SSA before and after chemical digestion by different acids (generic labelling); SSA: untreated, original sewage sludge ash, HCl: residue after SSA digestion with HCl; FSC-HCl: residue of HCl digestion of thermochemically treated SSA. Shares of material given in area-%.

When untreated and treated samples are compared, some of the material is missing. This material has been fully digested and moved to the liquid part. Analysis of the raw phosphoric acid showed other elements as well [11]. Wherever material has been removed in significant amounts, the proportion of other components changes. Upon closer investigation, three “key” spectra were identified. They represent the main P-bearing components of this SSA and are fully digested using HCl.

3.1. Insights Gathered by Generic Labelling

Using generic labelling [16], the spectra names are CaFeSiAlPO, CaPAlSiMgFeKO and PCaAlSiFeMgO. They contain 6, 12 and 16 wt% P, respectively, as determined by EDX analysis, and account for about 40 area-% of the material. By generic labelling, the first two of these would have ended up in the Ca-dominant group, and only the third as part of the P-rich material. Thus, when tracking P department, it is helpful to label spectra according to their P-content rather than the most abundant element.

3.1.1. CaSO₄

SSA contains calcium sulphate. HCl digests this initial SSA component. This material is commonly found around the edges of angular silicate particles, forming narrow rims (max ~30 µm) around grains. In terms of particle formation within the thermal process, this is interpreted as a result of condensation onto already formed particles. According to the mineral grain size distribution function of the MLA dataview software, this material has a typical D₅₀ of ~54 µm (grainsize at 50% of the cumulative passing grain size distribution curve).

3.1.2. Quartz and Other Silicates

Quartz is used as a fluidized bed in sewage sludge combustion, and is the only mineral reliably detected by XRD in these SSA. Since the acid used is unable to digest quartz, the initial amount of quartz should be preserved. For HCl digested residue, the compositional variance is within the normal variation of this material—a mode between 26 and 29 area-% (original SSA: mode of quartz 27 area-%). The spectra grouped as “other silicates” all contain Si as the major component, meaning no other measured element is more abundant within this spectrum. Still, within this group, the measured Si content varies between 7 and 32 wt% and averaging 23 wt% of the mode. “Other silicates” reach a slightly lower D_{50} (~98 μm) than quartz (~140 μm). “Other silicates” tend to be porous, rounded, amoeboid particles whereas quartz particles are more angular and lack pores.

3.1.3. Ca-Dominant Material

Material, in which Ca is the main component, is reduced from 7 area-% in SSA to 1 area-% in digestion residues. Spectra in this group contain an average of 27 wt% Ca. This material reaches a D_{50} of about 50 μm . It is found both as part of narrow rims around larger quartz and other silicate particles as well as porous, amoeboid, particles in conjunction with other silicates or phosphates. This material rarely forms particles with Al- or Fe-dominant material, an observation which encourages the interpretation that the thermal reorganization of SSA material is incomplete: phosphates are precipitated using Al- and Fe-salts during the wastewater treatment process. Since Al- and Fe-ions are unwanted in the recovered phosphoric acid, one goal of sewage sludge incineration for P-recovery is reorganizing the P-content into calcium-phosphates. However, the majority of spectra in this group are not only Ca-dominant but also contain Si, Al, and Fe.

3.1.4. High P-Material (>14 wt% P)

The residue still contains some remnants of P-rich material. Nonetheless, the content was greatly decreased in comparison to the original material. Less than 1.4 area-% of these phases remain, mostly the spectrum named as FePMgO. This residual P-content is rendered as acid-accessible by thermochemical pre-treatment, as was concluded by its absence in thermochemically pre-treated residue. Using the initial generic labelling, this material would have ended up in other groups, the aforementioned spectrum in Fe-rich material, for example. At a D_{50} of 90 μm , these particles are among the larger ones within the material, and they do form particles on their own, but often with the fully recoverable 3 key phases, silicates and Ca-dominant material. One of the spectra in here is Fe-P-O, a product of the precipitation of phosphates using Fe-salts during the wastewater treatment process. This material on its own has a D_{50} of 40 μm and usually forms particles with one of the 3 key spectra or other high P-material, a product of the incomplete thermal reorganization of phosphates during incineration.

3.1.5. Fe- and Al-Rich Material

These material components are formed during phosphorus removal in sewage treatment plants. Using iron and/or aluminum salts, phosphorus compounds precipitate and are preserved during incineration. Some of these only slightly soluble compounds even survive acid treatment, which is why these components appear relatively enriched in the residues. The residue shows an enrichment in Fe-phases compared to SSA. Residues will always represent an enrichment in phases which are hard to digest. As already mentioned, this SSA is contaminated with heavy metals and does not comply with the German fertilizer ordinance [19]. To address this issue, thermochemical pre-treatment was carried out. It was found that this treatment also improved P-recovery [9], which is why this process step was studied in the present experiments testing another acid. Less than 0.1 area-% of the three P-rich (14+ P) spectra remain. Fe-rich material was removed during pre-treatment, thus, reduced contents of this group are not surprising (by calculated assay, Fe content was roughly halved, 13.4 to 6.35 wt%).

All apparent increases in components in these residues are relative increases as more material has been digested. Particle sizes for these groups vary; at a D_{50} of $\sim 100 \mu\text{m}$, the Al-rich material is much coarser than Fe-oxides (D_{50} of $\sim 45 \mu\text{m}$). Fe-rich material typically appears as grains within larger, host particles of almost all other groups, the two exceptions being CaSO_4 and high P-material. Al-rich material follows the same trend.

3.1.6. HCl Digestion of Thermochemically Pre-Treated SSA

Comparing the pre-treated residue to the untreated residue, the Al-rich material and silicate material proportions rise. Fractions of Fe-rich, Ca-rich and residual high P-material decrease, the latter almost disappearing (0.02 area-%). P-recovery was more successful and pre-treated digestion residue contains less P (by calculated assay, about 0.5% less—1.08 wt% P remain). This highlights the need for an improved data evaluation—if as much P as possible is to be recovered, the current approach does not necessarily help process evaluation.

3.2. Insights Gathered by Target Grouping of EDX-Spectra

When applying the target grouping (P), compositions appear slightly different (Figure 3). All spectra are now sorted according to their P-content. If there was no P detected in the spectrum, it was labelled as before, by dominant (most abundant element within the spectrum). Thus, values for CaSO_4 are not affected by the new grouping procedure, since it does not contain P.

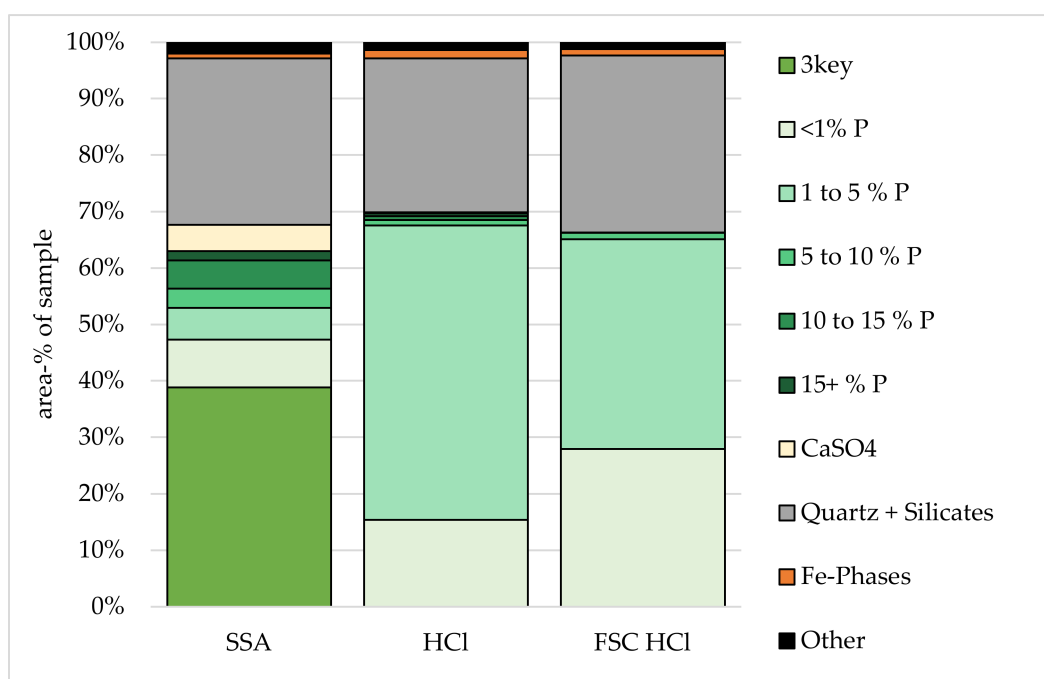


Figure 3. Composition of SSA before and after digestion with different inorganic acids evaluated with the target phase grouping procedure.

3.2.1. Quartz and Silicates

The distribution of quartz and silicates (quartz + silicates) remains in the same range as quartz in generic grouping. Here, generic labelling is expected to yield lower values, as the generic strategy distinguishes between “other silicates” and “quartz”. The target grouping combines the two, wherever they are P-free. Hence, whenever values for target quartz + silicates are lower than generic “quartz” and “other silicates” values, the Si-dominant material is P-enriched.

3.2.2. P-Containing Material

Residue content of P-phases digestion with HCl is only significant for the <5 wt% P spectra (groups < 1 and 1–5 wt% P). For spectra with a P-content of more than 15 wt%, the contents are reduced in residues (as compared to original SSA content). Although it looks like the fraction has the same extent as in the original material, taking into account that at least ~40 area-% of SSA were removed, reveals that these values represent a decrease beyond proportion. These material phases must have been particularly acid-accessible. In other words, among the P-containing groups, the original material has the largest share in 5–10 wt% P. Digestion shifts proportions, and in residues, the largest group among the P-containing groups is 1–5 wt% P. While the conventional grouping showed that high P-phases are severely depleted, target phase grouping highlights that the mid-level P-containing groups (quantitative relevance in the material) are also shifted towards lower P-values. Therefore, digestion acts on more P-containing species than just the high P-containing ones.

Phosphate content in SSA was depleted by 86 wt% [11]. This is shown by XRF analyses, since MLA studies cannot supply this information. There is the “Calculated Assay” operation within the MLA software in complex materials such as SSA, however, these values are better understood as a proxy.

The 10 to 15 wt% P-phase group is very accessible by the acid; they have been reduced from ~34 to <1.8 area-%.

3.2.3. Fe-Rich Material

Compared to the original material, Fe-phases have been depleted. Comparing these findings with generic labelling, some of the Fe-phases (generic) must contain phosphorus. Thus, they are not part of Fe-phases group (target phase). Target phase grouping thereby highlights that iron phosphates (generated in phosphate precipitation in wastewater treatment plants) are highly stable and not easily acid-accessible.

3.2.4. Residues of Pre-Treated Digestions (Target Grouping)

Pre-treatment led to an interesting shift in material phases. While the calculated assay values for P increase from SSA to pre-treated SSA (relative increase, as CaSO₄ is removed), the share of material components containing more than 10 wt% P decreases. At the same time, the amount of key spectra rises by about 10 area-%. Thus, the improved P-recovery after thermochemical pre-treatment is explained: thermochemical pre-treatment led to the formation of accessible material (see also [11]).

3.2.5. HCl Digestion

Comparing the pre-treated residue to the untreated residue, silicate and <1 wt% P proportions rise. Fractions of all other materials decrease. This implies that HCl digestion performs even better on pre-treated ash. This is also reflected in the images of treatment residues (Figure 3).

3.2.6. Generic Labelling

Prior to digestion, the P-phases were preferentially associated (30% binary) to quartz. In the residues (after digestion of pre-treated SSA), quartz phases are preferentially associated with other silicates, but mostly liberated. As they were mostly liberated in the original material, there is not much change here. Digestion is assumed to have worked as expected and >14 P-material was almost completely leached.

3.3. Target Evaluation

The fraction of liberated grains decreases for quartz + silicates by about 20%. In all P-containing phases, locking increases drastically (up to 98%) in all inorganic acid residues. Contrasting, in the original material, these groups were much more liberated, by up to 55%. The same is true for Fe-phases,

although the original degree of locking was higher in this group (75% up to 97%). Comparing locking values for quartz + silicates of pre-treated digestion residues with non-pre-treated digestion residues, these grains reveal reduced degrees of locking in residue (successful digestion of grains previously associated with quartz + silicates) for HCl. Thus, pre-treatment enables access to complex particles where access is desired. Quartz + silicates locking values for their preferred partner (1–5 wt% P-phases) show a decrease in locking values (pre-treated ash yields a residue with less complex quartz + silicates particles).

Locking increases in all phases between original SSA and residue. This lends room to the hypothesis of complex mechanisms leading to ternary⁺ particles. Keeping in mind that about 40 wt% of the material were already extracted, it is not surprising to find complex particles in the undigested residue.

4. Discussion

Within the literature studying SSA for P-recovery, it has been mentioned that the phosphate content is present as whitlockite [3–7]. The data presented here cannot confirm this. Whitlockite is easily acid-accessible, but none of the recovered material (as represented by the spectra that are present in the original material, but missing from the residue) show good agreement with the material studied here. By generic labelling, whitlockite would appear as PCaMgFeO, and at 20% P-content, fall into the >15 % P group of our target grouping. Neither an appropriate spectrum nor the majority of the P-content of this material in the >15 P group are found here. This is in agreement with other SSA studies [20].

This work suggests grouping EDX-spectra found in SEM-AM investigations of SSA for P-recovery by P-content. As shown, grouping them by their main component is less helpful when assessing the elemental department of phosphates and recovery success. Both options, however, show important characteristics for P-recovery. With regards to incineration, the reorganization of P-phases from those generated during P-precipitation in wastewater treatment to those present in ashes does currently not favor a clean recovery of calcium-phosphates. Thus, studies such as these can help assess different combustion regimes and their suitability towards P-recovery. With regards to P-recovery processes, an SEM-AM investigation reveals why recent works of P-recovery always had to deal with Al, Fe, and other macro elements in their process [8,21].

Particle sizes of the groups identified in this work are subject to the error of density settling of material during sample preparation and should be taken as “relative to each other”—this effect should affect all samples alike. Sawing up prepared epoxy blocks of the sample and turning the bands 90°, then analyzing them could show the extent of this error. A comparative study could potentially quantify this effect.

The generic labelling used in [9] allowed for the sorting of spectra by their main component, however, oftentimes material phases found in SSA are very complex and the “main” component is only “major” over other components by a few percent. Thus, the focus on P—as the target constituent which should be extracted—expresses itself in the target grouping. This data evaluation shows the extent to which remnant P-phases are still present in residues and the quality of SSA; a larger proportion of material containing relatively high levels of P is better suited than high levels of overall P-content. This P-recovery quality assessment cannot be done by XRF analyses, which determine the overall P-content of the material or XRD studies, where signals are overlain by a large scatter of random directions due to the large amorphous part of SSA. EDX data as obtained from a polished surface from a multitude of mapped grains, are a suitable method. To accentuate, three spectra were found which are exclusively present in the untreated material. These three spectra, named “key”, were completely digested by HCl, regardless of thermochemical pre-treatment of the digestion. In addition, this is the reason why thermochemical treatment resulted in an improved P-recovery: thermochemically treated SSA contained more key material, i.e., was able to generate key material. While other P-containing material phases varied in their response to treatment and thermochemical pre-treatment, these three phases always vanished completely, highlighting the P-recovery success of acid digestion.

It has been shown that generic labelling data evaluation [9] is limited when analyzing the P-contents of residues. A reduction in P-content in the residue is shown—the proportion of spectra containing less P rises, while the fraction of spectra containing more P decreases. Only half of this is illustrated by the conventional grouping: here, high P-phases are seen to vanish, but the rise of reduced P-species is not documented. The shift from 5–10 wt% P to 1–5 wt% P by simple digestion and to <1 wt% P in digestion after pre-treatment is obvious. This may be interpreted as the result of one of two processes: the material is removed, and thus, the relative proportion of remaining components rises—so, there is no actual enrichment; or the extraction mechanism by acid digestion only recovers a part of the P-content and not the full amount. In the latter case, it would be likely for new, mildly P-bearing spectra to appear in the residue but not in SSA. Since the same list of spectra was applied to all samples, this would either show certain spectra only present in residues or a significant increase in “unknown” material in residues. Neither is the case. Thus, there are shifts, triggered by the processes, but no generation of distinct phases. While the benefit of thermochemical pre-treatment is also visible using conventional grouping, it looks only marginal: digestion residues contain <5 area-% of the spectra with high P-content, and pre-treated show none. Using the target grouping, it is obvious that thermochemical pre-treatment affects more parts of the sample than specifically the heavy metal content only. The aforementioned shift in P-phase contents becomes visible. Fe-oxides are extracted by thermochemical pre-treatment.

As has been outlined in mathematical approaches (e.g., [22,23]), it is difficult to give estimates on uncertainty and error based on automated SEM mineral liberation analyses. The primary signal of MLA measurements is a backscattered electron image and energy dispersive spectra composed of data from numerous detector channels. The latter signal is based on ~12,000 counts gained within 10 ms. There is no specific time or channel resolution which could allow uncertainty and error estimates based on peak-to-background ratios and standard deviations for counting rates for distinct peaks. In consequence, for further estimates, the mineral mode appears as the most prominent parameter in comparison to the particle and grain sizes and their shape geometries.

During the preparation of the grain mount block, particle separation may be induced by the stirring of the particles into the liquid epoxy and subsequent gravitational subsidence of high-density particles during epoxy hardening. These effects can lead to heterogeneous particle distributions in the surface of a polished block, an effect that is particularly prominent for sample materials (mineral mixtures) with large differences in particle sizes and/or densities. As all samples thus prepared are affected by this bias towards particle distribution, it is suggested to study more than one sample—SSA and digestion residue, for example, or two types of SSA.

There are also uncertainties related to spectra classification. The EDX spectra classification algorithm for the MLA software packages follows the principle of best match along a scale of reliability between 1×10^{-10} (absolute conformance) to 1×10^{-100} (no conformance), as outlined by [10]. The phosphorus-bearing particles display a comparably complex pattern of X-ray emission lines, with many peaks and sub-peaks that are marked by considerable interference. Due to the complex X-ray spectra characteristics, there is considerable risk that EDX spectra are not at all classified, if classification is carried out at a high reliability value. The classification algorithm allows no alternative assignment to another EDX reference spectrum or to another mineral in the list. Due to this principle, the spectra which cannot be classified by the higher reliability scale value will remain as unknown and increase the mode of unknown grains [11]. For the study presented here, the sample EDX spectra were thus classified by the reliability values of 1×10^{-10} (high degree of conformance) and 1×10^{-25} (fair degree of conformance). The latter reliability value is applied to process samples, in an effort to reduce the amount of unknowns below 0.1 area-% mode. Applying a reliability value of 1×10^{-25} to the samples of the third case study, the modes of unknowns remained low, ranging between 0.53 and 0.16 area-%.

5. Conclusions

This study defined the three P-containing phases in SSA which are completely recovered by HCl acid digestion. This implies that the recoverable P-content of SSA studied (sludge burned at 850 °C) lies not in a single mineral phase, but in multiple element associations. Any recovered phosphorus product from SSA will inevitably require costly purification. At the same time, acid digestion does not recover the full P-content. Legal obligations to recover the full content are likely to result in economic actors not pursuing P-recovery from SSA at all. Thus, several routes are probable: SSA not being used for P-recycling (too costly), legal requirements being adjusted or SSA being optimized—perhaps the P-content can be reorganized in easily recoverable phases by optimizing the combustion regime. Workers with SSA combusted at higher temperature report less elementary complex phases, and our work shows that higher P-phases are composed of fewer elements. Thus, the impurities in recovered phosphoric acid that need to be stripped off are reduced in complexity. Future work could address SSA from different wastewater treatment plants incinerated at the same furnace to shed light on P-department. This would enable the study of provenance effects and should help to differentiate between incineration- and provenance-based effects. Another possible route would be P-recovery prior to incineration, yet this work focused on developing a new spectra naming/grouping strategy for SSA, which is recommended to use during future work for advancing this particular area of waste management.

P-recovery from SSA should, ideally, start with exploring a combustion regime that optimizes P-phase shift towards recoverable P-phases with fewer elements. This study showed that higher P-content in material phases is accompanied by fewer elements. Future work could focus on improving combustion for an efficient P-recovery from SSA.

Author Contributions: Following an idea of M.B., conceptualization by B.S. and M.B. was followed by V.-G.G. carrying out experiments. A.C.G. evaluated data and drew conclusions and proposed spectra labelling. Draft preparation and writing were done by A.C.G., M.B. and B.S. All authors have read and agreed to the published version of the manuscript.

Funding: This research was funded by the German federal ministry for economic affairs and energy, BMWi FKZ 03EFGSN097 and the German federal ministry of education and research, BMBF FKZ 033R099E. These were granted to M.B. and his institute.

Acknowledgments: The authors would like to thank Wirbelschichtfeuerungsanlage Elverlingsen GmbH for providing the samples. Furthermore, we are grateful for Sabine Gilbricht of the Geometallurgy Laboratory at the Department of Economic Geology and Petrology, TU Freiberg, for kindly supporting the MLA analyses. The authors would like to express gratitude towards the three anonymous reviewers whose comments improved this work.

Conflicts of Interest: The authors declare no conflict of interest.

References

1. European Commission. Communication from the Commission to the European Parliament, the Council, the European Economic and Social Committee and the Committee of the Regions on the Review of the List of Critical Raw Materials for the EU and the Implementation of the Raw Materials Initiative. Available online: <https://eur-lex.europa.eu/legal-content/EN/TXT/?uri=CELEX%3A52014DC0297> (accessed on 25 May 2020).
2. Werther, J.; Ogada, T. Sewage sludge combustion. *Prog. Energy Combust. Sci.* **1999**, *25*, 55–116. [[CrossRef](#)]
3. Fowlie, P.J.; Stepko, W.E. *Sludge Incineration and Precipitant Recovery*; Technical Report No 72-3-4; Pollution Control Branch, Ontario Ministry of the Environment: Toronto, ON, Canada, 1978.
4. Liu, Y.; Kumar, S.; Ra, C.; Kwag, J.-H. Magnesium ammonium phosphate formation, recovery and its application as valuable resources: A review. *J. Chem. Technol. Biotechnol.* **2012**, *88*, 181–189. [[CrossRef](#)]
5. Montag, D. Phosphorrückgewinnung bei der Abwasserreinigung—Entwicklung eines Verfahrens zur Integration in Kommunalen Kläranlagen. Ph.D. Thesis, RWTH Aachen University, Aachen, Germany, 2008.
6. Oliver, B.; Carey, J. Acid solubilization of sewage sludge and ash constituents for possible recovery. *Water Res.* **1976**, *10*, 1077–1081. [[CrossRef](#)]

7. Scheidig, K.; Lehrmann, F.; Mallon, J.; Schaaf, M. Klärschlamm-Monoverbrennung mit integriertem Phosphor-Recycling. In *Energie aus Abfall*, 1st ed.; Thome-Kozmiensky, K.J., Beckmann, M., Eds.; TK Verlag: Neuruppin, Germany, 2013; pp. 1039–1046.
8. Ottosen, L.; Jensen, P.E.; Kirkelund, G.M. Phosphorous recovery from sewage sludge ash suspended in water in a two-compartment electro-dialytic cell. *Waste Manag.* **2016**, *51*, 142–148. [[CrossRef](#)] [[PubMed](#)]
9. Greb, V.G.; Guhl, A.; Weigand, H.; Schulz, B.; Bertau, M. Understanding phosphorus phases in sewage sludge ashes: A wet-process investigation coupled with automated mineralogy analysis. *Miner. Eng.* **2016**, *99*, 30–39. [[CrossRef](#)]
10. Greb, V.-G.; Fröhlich, P.; Weigand, H.; Schulz, B.; Bertau, M. Phosphatrecycling aus Klärschlammaschen—Warum Phosphorsäure der Königsweg ist. In *Rohstoffwirtschaft Und Gesellschaftliche Entwicklung—Die Nächsten 50 Jahre*, 1st ed.; Kausch, P., Matschullat, J., Bertau, M., Mischo, H., Eds.; Springer: Heidelberg, Germany, 2016; pp. 154–196.
11. Greb, V. Rückgewinnung Von Phosphor Aus Klärschlammaschen Durch Sauren Aufschluss Unter Berücksichtigung Einer Thermischen Vorbehandlung. Ph.D. Thesis, TU Bergakademie Freiberg, Freiberg, Germany, 2018.
12. Fandrich, R.; Gu, Y.; Burrows, D.; Moeller, K. Modern SEM-based mineral liberation analysis. *Int. J. Miner. Process.* **2007**, *84*, 310–320. [[CrossRef](#)]
13. Smith, D.G.W.; De St. Jorre, L. The MinIdent Data Base—Examples of applications to the Thor Lake rare metal deposits. In Proceedings of the Abstracts with Program, 14th General Meeting of International Mineralogical Association, Stanford, CA, USA, 13–18 July 1986; p. 234.
14. Gu, Y. Automated scanning electron microscopy based mineral liberation analysis an introduction to JKMR/FEI mineral liberation analyser. *J. Miner. Mater. Charact. Eng.* **2003**, *2*, 33–41.
15. Lastra, R. Seven practical application cases of liberation analysis. *Int. J. Miner. Process.* **2007**, *84*, 337–347. [[CrossRef](#)]
16. Schulz, B.; Merker, G.; Gutzmer, J. Automated SEM Mineral Liberation Analysis (MLA) with Generically Labeled EDX Spectra in the Mineral Processing of Rare Earth Element Ores. *Minerals* **2019**, *9*, 527. [[CrossRef](#)]
17. Ayling, B.; Rose, P.; Zemach, E.; Drakos, P.; Petty, S. QEMSCAN (Quantitative Evaluation of Minerals by Scanning Electron Microscopy): Capability and application to fracture characterization in geothermal systems. *AGU Fall Meet. Abstr.* **2012**, 1158. [[CrossRef](#)]
18. Ma, Y.; Stopic, S.; Gronen, L.; Friedrich, B. Recovery of Zr, Hf, Nb from eudialyte residue by sulfuric acid dry digestion and water leaching with H₂O₂ as a promoter. *Hydrometallurgy* **2018**, *181*, 206–214. [[CrossRef](#)]
19. DüMV, Verordnung über das Inverkehrbringen von Düngemitteln, Bodenhilfsstoffen, Kultursubstraten und Pflanzenhilfsmitteln (Düngemittelverordnung—DüMV), 5 December 2012, BGBl. I, 2482 last amendment by article 1 of the ordinance of 27 May 2015, BGBl. I, 886. Available online: https://www.gesetze-im-internet.de/d_mv_2012/D%C3%BCMV.pdf (accessed on 25 May 2020).
20. Pavón, S.; Guhl, A.C.; Pätzold, C.; Bertau, M. Verfahren zur Behandlung von Flugasche und Ascherückstand zur Phosphorsäuregewinnung. In Proceedings of the 1st Annual abonocare@Conference, Leipzig, Germany, 18 March 2020.
21. Fang, L.; Li, J.-S.; Donatello, S.; Cheeseman, C.; Wang, Q.; Poon, C.S.; Tsang, D.C. Recovery of phosphorus from incinerated sewage sludge ash by combined two-step extraction and selective precipitation. *Chem. Eng. J.* **2018**, *348*, 74–83. [[CrossRef](#)]
22. Leigh, G.; Sutherland, D.; Gottlieb, P. Confidence limits for liberation measurements. *Miner. Eng.* **1993**, *6*, 155–161. [[CrossRef](#)]
23. Tolosana-Delgado, R.; Mueller, U.; Boogaart, K.G.V.D. Geostatistics for Compositional Data: An Overview. *Math. Geol.* **2018**, *51*, 485–526. [[CrossRef](#)]

